Human macrophage adhesion on polysaccharide patterned surfaces

ARTICLE *in* SOFT MATTER · MARCH 2011

Impact Factor: 4.03 · DOI: 10.1039/C0SM01353F · Source: PubMed

6 AUTHORS, INCLUDING:

Stanley J Stachelek
The Children's Hospital of Philadelphia
27 PUBLICATIONS **545** CITATIONS
SEE PROFILE

David M Eckmann
University of Pennsylvania
142 PUBLICATIONS **1,658** CITATIONS
SEE PROFILE

Soft Matter

View Online
Dynamic Article Links

Cite this: *Soft Matter*, 2011, **7**, 3599

www.rsc.org/softmatter

PAPER

Human macrophage adhesion on polysaccharide patterned surfaces

Irene Y. Tsai,[b] Chin-Chen Kuo,[b] Nancy Tomczyk,[a] Stanley J. Stachelek,[c] Russell J. Composto[b] and David M. Eckmann*[a]

Received 21st November 2010, Accepted 1st February 2011
DOI: 10.1039/c0sm01353f

Despite many advances in designing biocompatible materials, inflammation remains a problem in medical devices and implants. We report two methods, microcontact printing and photodegradation by UV exposure, to pattern dextran and hyaluronic acid on glass, as well as demonstrate their utility for use as an anti-inflammatory biomaterial. The dextran/glass patterned surface can be further modified by grafting hyaluronic acid to glass, creating a binary polysaccharide patterned surface. We used two geometries, 90 μm squares and 22 μm stripes, to study the human macrophage (THP-1) adhesion on the patterned surfaces containing dextran, hyaluronic acid and the binary pattern. The results indicate that a majority of the macrophages are non-adherent on hyaluronic acid for three day culture. The ranking of surfaces according to macrophage adhesion is 3-aminopropyltriethoxysilane-modified glass culture dish, dextranized surfaces, glass, and hyaluronic acid-modified surfaces. On the binary pattern of dextran and hyaluronic acid, macrophages preferentially attach and adhere to the dextranized area. Patterned surfaces provide an excellent platform for mimicking the complexity of the glycocalyx and investigating the interface between this surface and cells. This binary polysaccharide pattern also offers a new route to address anti-inflammatory potential of surface coatings on biomaterials in a high through-put fashion.

Introduction

The endothelial glycocalyx layer is the surface layer of the vascular endothelium. This layer consists mostly of carbohydrates and has several important functions such as regulating the vascular permeability,[1,2] acting as a mechanotransducer[3] and balanced signaling events in the local microenvironment.[4] During inflammation, the glycocalyx layer has been shown to degrade to facilitate leukocyte recruitment.[5,6] Conversely, an undamaged layer inhibits a cascade of inflammatory events, and thus, mimicking the endothelial glycocalyx surface can be a route to reduce inflammation caused by medical implants and devices.[7] Here, we report the adhesion of the human macrophage cell line, THP-1, on surfaces presenting immobilized dextran, hyaluronic acid, patterns of dextran and hyaluronic acid on glass, as well as binary patterns of dextran and hyaluronic acid. These surfaces profile a model platform for better understanding the anti-inflammatory potential of the glycocalyx.

Because the endothelial glycocalyx layer is heterogeneous, composed of different polysaccharides,[5] and rough, it is conceivable that the spatial organization of the polysaccharides and the topography play an important role in the adhesion of macrophages, and consequently, their inflammatory responses. Wójciak-Stothard *et al.*[8] studied P388D1 macrophages on microfabricated grooves (30 to 282 nm) and found that cytoskeletal organization and focal adhesion depended on the nano-sized features. They also found more phagocytotic activity on the patterned surfaces than fused silica substrata.[8] In addition, Zhang's group found mouse macrophages adhere only to the gold regions of a surface patterned with PEG.[9]

Anderson's group has several studies using human peripheral blood monocytes on surfaces of different hydrophilicity and charges,[10] as well as photochemically micropatterned surfaces.[11] This group found that significantly more adherent macrophages experience apoptosis on the hydrophilic and anionic surfaces than the hydrophobic or the cationic surfaces *in vitro*[12] and *in vivo*.[13] In terms of cytokine responses, Brodbeck *et al.*[12] showed human macrophages express more interleukin-10 (anti-inflammatory) and less interleukin-8 (pro-inflammatory) on hydrophilic and anionic surfaces, respectively, indicating that surface modification is directly related to the inflammatory response. While these experiments confirm the importance of surface chemical heterogeneity and surface topography on macrophage adhesion and activity, few experiments examine how surface coating containing the molecular constituents of the endothelial glycocalyx can reduce inflammatory responses provoked by biomaterials. In this study, we vary the spatial distribution of the

[a]*Department of Anesthesiology and Critical Care, University of Pennsylvania, Philadelphia, PA, 19104, USA. E-mail: eckmanndm@uphs.upenn.edu; Fax: +1 215 349 5078; Tel: +1 215 349 5348*
[b]*Department of Materials Science and Engineering, University of Pennsylvania, Philadelphia, PA, 19104, USA*
[c]*Department of Pediatrics, University of Pennsylvania, Philadelphia, PA, 19104, USA*

dextran and hyaluronic acid on a surface by using microcontact printing and photochemical micropatterning to investigate human macrophage adhesion. Insights from these studies can lead to improved coatings that reduce inflammation on medical implants, biosensors and other medical devices.

Surface patterning has become an important route to fabrication of many biomedical technologies such as biosensors,[14] smart biomaterials,[15] tissue engineering[16] and microfluidic devices.[17] Several techniques are available to pattern a surface having nano- to micron-size topographies, differing degrees of hydrophobicity and various biomolecular ligands. In particular, microcontact printing and photochemical micropatterning are facile techniques that do not require elaborate cleanroom facilities. Microcontact printing has been used widely to pattern proteins,[18,19] polysaccharides,[20,21] DNA[22] and cells.[23,24] For example, Zhou *et al.* used microcontact printing to pattern tetraoctadecylammonium bromide on carboxymethylated dextran hydrogels for protein microarray applications.[25] Furthermore, surface patterning of hyaluronic acid on a poly(ethylene terephthalate) film has been shown to be effective in antithrombogenicity.[26] Others have used photochemical micropatterning to pattern proteins by photodegradation of a poly(oligo(ethylene glycol) methacrylate) brush.[27] Lu *et al.*[28] studied cell adhesion of fibroblasts and immortalized cancer cells on patterned polyelectrolyte multilayers manufactured using a room-temperature imprinting method and demonstrated that the local geometry of patterned stripes (*e.g.*, height and width) regulates cell attachment.

Although microcontact printing appears to have become a routine method[18–25] the combination of pattering HA and dextran has not previously been achieved and is demonstrated successfully herein. This has particular significance for vascular biology applications specifically because these two different polysaccharides are primary components of the endothelial cell glycocalyx layer which is in direct contact with circulating blood. We used microstamping and photodegradation methods to fabricate five different patterned surfaces, namely (1) dextran and glass (dextran/glass), (2) hyaluronic acid and glass (hyaluronic acid/glass), (3) dextran and 3-aminopropyltriethoxysilane-modified glass (dextran/APTES-glass), (4) hyaluronic acid and APTES modified glass (hyaluronic acid/APTES-glass), as well as (5) dextran and hyaluronic acid (dextran/hyaluronic acid). We also used exemplars of patterned surfaces to study related cell adhesion interactions with macrophages.

To study macrophage adhesion, we chose patterned surfaces generated by the photodegradation method. Patterned surfaces of rhodamine-dextran/glass, fluorescein-hyaluronic acid/glass and rhodamine-dextran/hyaluronic acid were used to investigate how micrometre-sized patterns direct macrophage adhesion. The patterned surfaces were characterized by fluorescence microscopy and atomic force microscopy, and their corresponding surface chemistries were also verified with contact angle and ellipsometry measurements of the homogeneous surfaces. To understand the macrophage adhesion on patterned surfaces, we quantified the macrophage spreading area on a homogeneous surface of dextran (or rhodamine-dextran), hyaluronic acid (or fluorescein-hyaluronic acid), glass, APTES-glass and culture dish. We found that macrophages have the highest spreading area on APTES among the surfaces we studied, followed by culture dish, dextran, glass and hyaluronic acid surfaces. This result is consistent with the patterned surfaces. In particular, the binary polysaccharide surface consisting of dextran and hyaluronic acid shows that macrophages preferentially adhere to the dextranized regions. This patterned surface can be used as a model to understand the interaction between the macrophages and the endothelial glycocalyx surface. Furthermore, this preferential non-attachment and non-spreading onto the hyaluronic acid can be exploited to surface-direct cellular responses in applications for medical devices and therapeutic and diagnostic tools.

Experimental

Materials and methods

All solvents and reagents were utilized as received. 3-Aminopropyltriethoxysilane (APTES), sodium periodate ($NaIO_4$), sodium cyanoborohydride ($NaBH_3CN$), 1,6-diaminohexane, dimethylformamide and HEPES were purchased from Sigma-Aldrich Co. and Fisher Scientific. Dextran is from *Leuconostoc mesenteroides* with molecular weight of 64 000–76 000 (Sigma #D4751). Hyaluronic acid has a molecular weight of 750 000 (Sigma #H1504). For fluorescence imaging, rhodamine B isothiocyanate-dextran (Sigma #R9379, M_w = 70 000) and fluorescein hyaluronic acid (Sigma #F1177, M_w= 800 000) are used. 1-Ethyl-3-(3-dimethylaminopropyl)carbodiimide hydrochloride (EDC) and sulfo-NHS were purchased from Thermo Fisher Scientific, #22980 and #24510, respectively. Sylgard 184 Silicone elastomer curing agent and elastomer base were purchased from Dow Corning to make poly(dimethylsiloxane) (PDMS) stamps. Silicon oxide surfaces were purchased from Silicon Quest International (Santa Clara, CA). Two different TEM grids were used, Electron Microscopy Science, Cat# G200-Cu and Cat# G400P-Ni.

Microcontact printing on glass or PU films

The PDMS stamp was prepared by casting the mixture of elastomer curing agent and elastomer base (ratio 1 : 10) against a patterned silicon wafer (master). The master patterned surface (silicon) consists of 10 μm stripes. Oxidized rhodamine dextrans were prepared using the same procedure described in a previous publication.[29] A drop of oxidized dextran (100 μL) was pipetted onto the patterned surface of the PDMS and covered for 1 hour. For fluorescence imaging, rhodamine dextran was used in place of dextran. Dextran was then removed from the patterned surface and let dry for 1 minute before stamping the patterns onto an aminated glass or an aminated PU film. The glass or a PU film was aminated *via* APTES or 1,6-diaminohexane, respectively. Gentle pressure was applied to the PDMS to make sure that the patterns were in contact with the substrate. The substrate was covered with aluminium foil overnight before the stamp was peeled away, yielding a surface having a pattern of rhodamine dextran/APTES-glass or dextran/NH_2–PU. The surface was rinsed several times with de-ionized water.

Photodegradation micropatterning on glass

Silicon wafers and glass coverslips were cleaned using "piranha" solution (70% H_2SO_4 and 30% H_2O_2, v/v) for 20 minutes at 80 °C

to ascertain a homogeneous silanol layer that could react with APTES. The surfaces were washed with water numerous times and dried in an oven. Upon a dried clean silicon surface, the silane APTES reaction was carried out immediately. The APTES thickness and contact angle were verified by ellipsometer (Rudolph AutoEL II) and contact angle goniometer, respectively. A TEM grid (EMS #G400P-Cu and G200-Cu) was used as a photomask. The APTES surface was exposed to UV for 7 minutes. The unmasked APTES regions were degraded by UV. This produced a silanol and amine functionalized patterned surface. The surfaces were washed with toluene and water several times.

The silanol/aminated glass substrates were immersed in aqueous oxidized dextran solution. The oxidation conditions and the extent of oxidation were studied previously.[29] Briefly, dextran solution (2 mg ml^{-1}) was prepared and oxidized using 1.5 gram of $NaIO_4$ in the reaction. After oxidizing for 1 hour, $NaBH_3CN$ (15 mg) was dissolved into the oxidized solution. The reaction was placed on an orbital shaker for 1 day. The dextran patterned surface was removed from the solution and washed with water several times. For hyaluronic acid patterning, a well established procedure, the EDC-mediated condensation with *N*-hydroxysuccinimide, was followed. Specially, the silanol/aminated glass substrate was immersed in a solution containing hyaluronic acid (2 mg ml^{-1}), EDC (38.2 mg ml^{-1}), sulfo-NHS (10.8 mg ml^{-1}) and HEPES (2.3 mg ml^{-1}) for 1 day at room temperature. After one day of reaction, the hyaluronic acid patterned surface was washed with water many times and dried using nitrogen gas.

Binary polysaccharide patterns

Subsequent to successfully patterning of dextran/glass or dextran/APTES-glass, hyaluronic acid (or fluorescein-hyaluronic acid) was immobilized onto the non-dextran regions (Fig. 1). The rectangular pattern of dextran on glass *via* photodegradation micropatterning or microcontact printing was immersed in hyaluronic acid (2 mg ml^{-1}), EDC, HEPES and sulfo-NHS, following a procedure described earlier. After two days of reaction, the dextran/hyaluronic acid patterned surface was washed with water many times and dried using nitrogen gas.

Surface characterization

Homogenous surfaces of dextran or hyaluronic acid were verified using contact angle and ellipsometry when appropriate. The fluorescence images were taken using an Olympus BX50 microscope to verify the success of the patterned surfaces. The patterned surfaces were characterized using scanning force microscopy (Veeco) in both dry (air) and wet (PBS buffer solution) conditions. The images were analyzed to obtain the degree of swelling for dextran and hyaluronic acid.

Macrophage culture

The human monocyte derived macrophage cell line, THP-1 (ATCC Manassas, VA), was grown in RPMI medium (Cell Culture Technologies, Herndon VA) supplemented with 5% fetal calf serum and 0.05 μM 2-mercaptoethanol. To assess inflammatory cell attachment to the patterned surfaces, the THP-1 cells were stimulated with the addition of 1.6 × 10^{-7} M phorbol 12-myristate 13-acetate[30] and seeded onto the modified surfaces at a concentration of 500 000 cells per ml. Macrophages were cultured on the substrates for 1, 2 and 3 days. Macrophages on the homogeneous surface were imaged using optical microscopy. For the patterned surfaces, an image of the patterned surface was taken, followed by macrophage image, and the two images were merged.

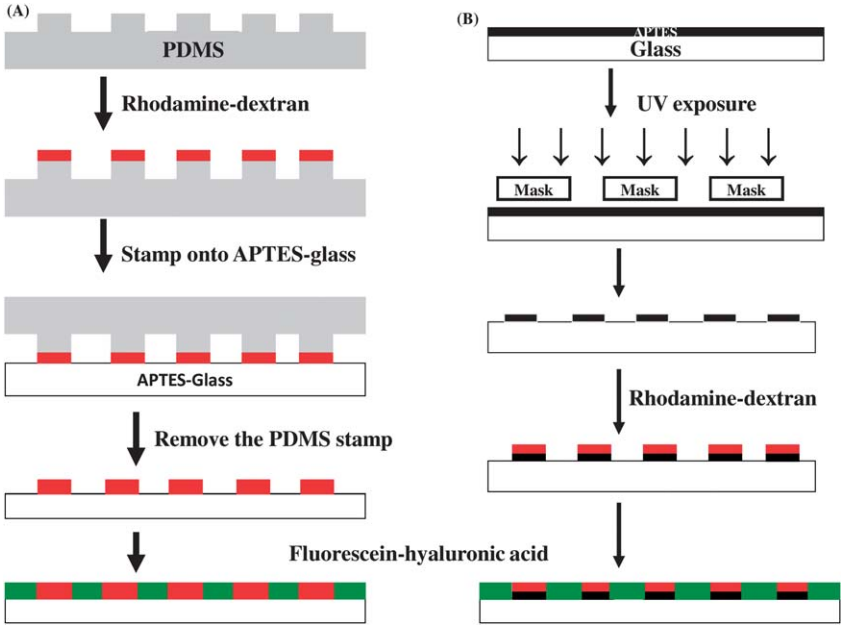

Fig. 1 Schematic representation of rhodamine-dextran patterns fabricated by (A) microcontact printing and (B) photodegradation of APTES and subsequently reacted with fluorescein-hyaluronic acid.

Cell spreading area analysis

Cells were photographed and evaluated for cell spreading area using bright field microscopy, using a Nikon Eclipse TE300 inverted fluorescent microscope. The data shown represent means and standard error of the mean (SEM) of three experiments and six fields. The number of cells analyzed was from 110 to 345 cells for each data point. Cell spreading area was analyzed using Image J software, downloadable from the National Institutes of Health. Statistical tests were performed using analysis of variance (ANOVA) with $p = 0.05$.

Results and discussions

Polysaccharide patterning and characterization

Prior to surface patterning, uniform homogenous surfaces of dextran, hyaluronic acid and APTES were made on silicon wafers and glass to verify the surface reaction. Surfaces were characterized by contact angle and ellipsometer as described in previous publications.[31] Briefly, silicon oxide surfaces are chemically modified to contain 3-aminopropyltriethoxysilane (APTES), and subsequently reacted with oxidized dextran or hyaluronic acid. The contact angles of APTES-, dextran- and hyaluronic acid-modified surface are $55 \pm 6°$, $35 \pm 2°$ and $21 \pm 5°$, respectively. On the silicon oxide surface, the average thicknesses of the APTES-, dextran- and hyaluronic acid-modified surface are 10 ± 1 Å, 9 ± 3 Å and 18 ± 4 Å, respectively. These data are consistent with previous results and other published values.[32]

The photodegradation and microcontact printing methods were successfully used to pattern rhodamine-dextran, fluorescein-hyaluronic acid and their combination on a surface. Fig. 1 shows the scheme for the fabrication process. The fluorescence microscopy images, Fig. 2A–C, demonstrate the success of the patterning for rhodamine-dextran/glass, fluorescein-hyaluronic acid/glass, and rhodamine-dextran/fluorescein-hyaluronic acid, respectively. Both methods do not require extensive equipment and can be carried out in biological laboratories. This is especially true using the photodegradation method since the masks can be purchased readily. Although both techniques can yield the same patterned sizes, the surface chemistries for the patterns are different. While the microcontact printing method results in rhodamine-dextran alternating with APTES-glass (rhodamine-dextran/APTES-glass), Fig. 2A, the pattern generated by photodegradation is a combination of rhodamine-dextran and glass. This is important because the APTES-glass is hydrophobic and glass is not. Similarly, the hyaluronic acid patterning results in fluorescein-hyaluronic acid/APTES-glass for microcontact printing, Fig. 2B.

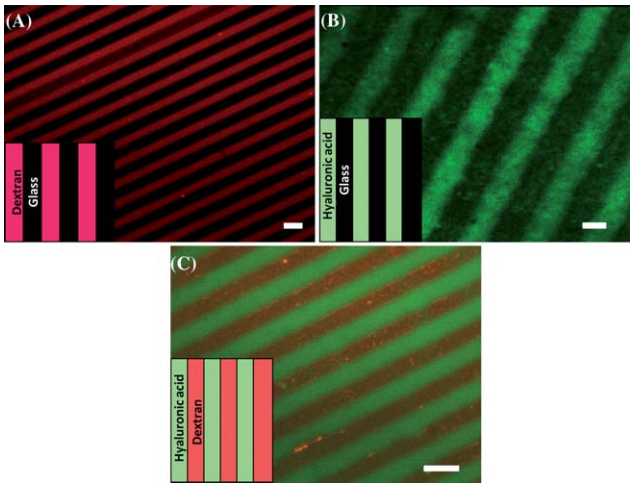

Fig. 2 Fluorescence images of three different patterns using microcontact printing, namely (A) rhodamine-dextran/glass, (B) fluorescein-hyaluronic acid/glass and (C) rhodamine-dextran/fluorescein-hyaluronic acid features. Scale bar length is10 μm.

After preparing the rhodamine-dextran/glass pattern, a second polysaccharide can be attached to the glass regions using the photodegradation method or the APTES-glass region using microcontact printing. In our study, we chose hyaluronic acid because it is native to human tissues as well as a constituent of the endothelial glycocalyx surface. Hyaluronic acid was tagged with fluorescein which emits green. The binary pattern of rhodamine-dextran and fluorescein-hyaluronic acid is shown in Fig. 2C using microcontact printing. The rhodamine-dextran/fluorescein-hyaluronic acid patterned surface can also be made using the photodegradation method. Fig. 3A is an image of the rhodamine-dextran and Fig. 3B is the fluorescein-hyaluronic acid. Merging the two images, we demonstrate that both polysaccharides form distinct regions corresponding to either rhodamine-dextran or fluorescein-hyaluronic acid.

In addition to fluorescence microscopy, the patterned surfaces made by microcontact printing were characterized using atomic force microscopy (AFM). Fig. 4A and B are tapping mode AFM images of patterned surfaces of dextran/glass and hyaluronic acid under dry and wet conditions, respectively. For this analysis we measured the stripes because the AFM scanning size is limited to

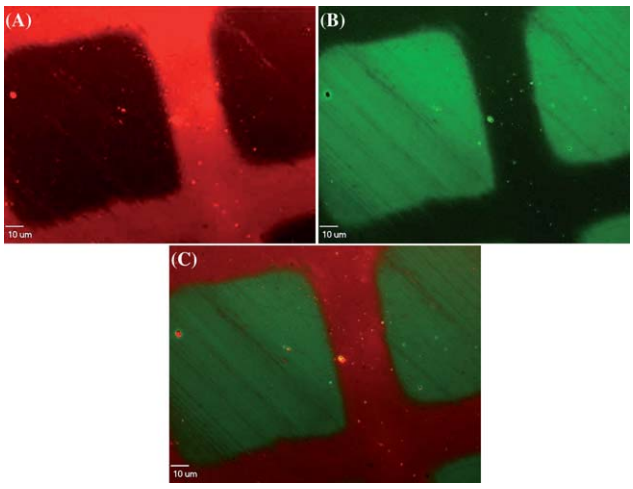

Fig. 3 Binary polysaccharide patterns of rhodamine-dextran (perimeter region)/fluorescein-hyaluronic acid (square core regions) prepared by the photodegradation method. (A) Fluorescence image of rhodamine-dextran using 535–585 nm excitation and 600–655 nm emission filters, (B) fluorescein-hyaluronic acid using 460–490 nm excitation and 515–550 nm emission filters and (C) the merged images from (A) and (B), showing both rhodamine-dextran and fluorescein-hyaluronic acid on one single patterned substrate.

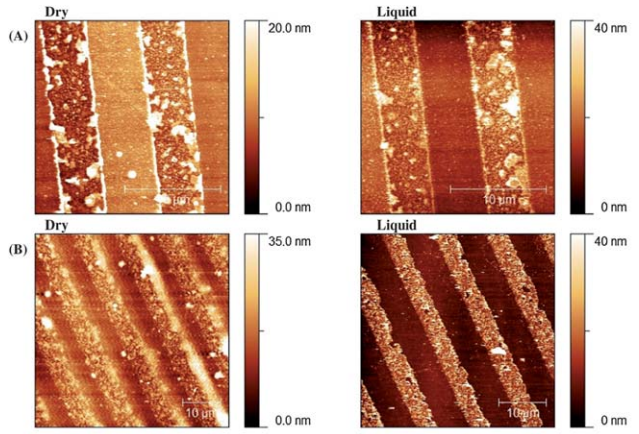

Fig. 4 AFM topography images of (A) rhodamine-dextran/glass and (B) fluorescein-hyaluronic acid/glass pattern taken in dry and in liquid tapping modes. The periodicity is 10 μm with 5 μm width for the polysaccharide regions. The dextran pattern shows patchy areas of dextran clusters, whereas the hyaluronic acid pattern has more uniform coating on the surface. Scale bar length is 10 μm.

~90 μm, which would give an incomplete view of the 90 μm square pattern used. AFM images reveal patches of dextran and hyaluronic acid across the surface coverage. The glass regions are relatively flat with roughness on the order of 1 nm, suggesting that polysaccharides do not attach to the glass. Consistent with the master pattern, the AFM images of the patterned surfaces show 10 μm periodicity with 5 μm width for the polysaccharide regions. The root mean square (RMS) values of the difference in the height irregularities were analyzed on the non-aggregate regions. The polysaccharide patches may have multiple polymer chains, and thus, these dextran or hyaluronic acid aggregates are not quantified. The RMS values of the Δ_{height} are 2.0 ± 0.5 nm and 3.5 ± 0.2 nm for the dextran pattern on glass under dry and wet conditions, respectively, where Δ_{height} is the difference between the height of the dextranized region and the height of the glass region. Similarly, for the hyaluronic acid pattern, the values of Δ_{height} RMS are 2.8 ± 0.2 nm and 6.9 ± 0.7 nm for dry and wet conditions, respectively. This degree of swelling is similar to that found by Ferrer *et al.* in recent experiments in which the polysaccharides swelled by 2–3 fold, depending on the hydrogen bonding.[33]

Both microcontact printing and photodegradation can yield micrometre-sized patterned surfaces. However, we found the photodegradation method to produce more consistent edges and borders. Preparation of reproducible patterned surfaces using microcontact printing requires much trial and error. Moreover, microcontact printing requires a master pattern on a silicon wafer which may not be easy to obtain. For these reasons, the photodegradation method was used to create patterns to study human macrophage adhesion.

Human macrophage adhesion on the homogenous surfaces

Macrophage spreading area was analyzed for each uniformly modified surface. Fig. 5A–E present representative images of macrophage morphology on surfaces of APTES, glass, culture dish, dextran and hyaluronic acid, respectively. On all the surfaces studied except hyaluronic acid, macrophages adhered and spread well, demonstrating distinct lamellipodial extensions. There were also subpopulations of macrophages on these surfaces which attached, but which did not spread significantly. The spreading cells took on elongated, polygonal or circular morphologies. On the hyaluronic acid surfaces, the adherent cells remained much smaller in their attachment and spread coverage area in comparison to the cells on the other surfaces. The macrophages on the hyaluronic acid-modified surfaces primarily remained rounded, and the cells also formed multi-cell clusters, unlike the cells on the other surfaces which remained spatially isolated from each other. The few cells that attached to the hyaluronic acid surface were lacking the spreading feature of large lamellipodia, but some cells did elongate in forming clusters with other cells.

In Fig. 6, cell spreading area was plotted as a function of the different types of modified surfaces. Comparing spreading that occurred on the hyaluronic acid-modified surface to that of the other surfaces studied, cell spreading was statistically

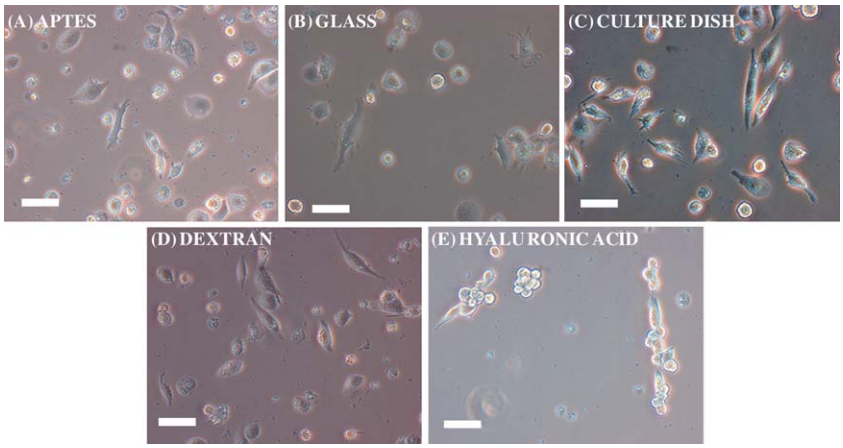

Fig. 5 Representative images of macrophage attachment and spreading on (A) APTES, (B) glass, (C) culture dish, (D) dextran and (E) hyaluronic acid for 3 days. The macrophages attach and spread well on APTES, glass, culture dish and dextran, except the hyaluronic acid surface. The cells that attached on hyaluronic acid form clusters, showing preference for cell–cell adhesion rather than cell–surface adhesion. Scale bar length is 50 μm.

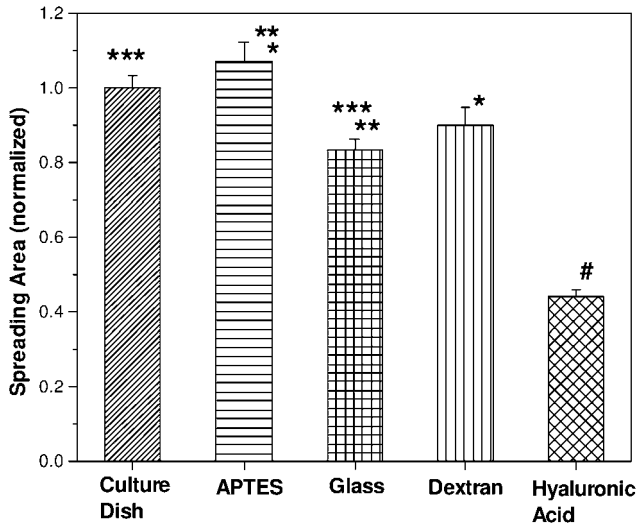

Fig. 6 Normalized macrophage spreading area analysis on various homogenous surfaces. Each bar represents the mean spread area of 110–345 cells of six fields in three experiments. Error bars indicate standard error of the mean (SEM). Statistical significance is for $p < 0.05$ using analysis of variance. Symbols (#), (*), (**) and (***) indicate statistically significant deviations from the hyaluronic acid surface, dextranized surfaces, APTES surface and glass, respectively.

significantly less than on each of the other surfaces. This indicates that the hyaluronic acid-modified surface presents far less favorable chemistry for macrophage adhesion than do dextran, glass, APTES-modified glass and culture dish surfaces. In addition, macrophages favored cell-to-cell interactions represented by formation of clusters of cells when adhering to hyaluronic acid, but not the other surface chemistries, as evidenced by the images in Fig. 5A–E.

The macrophage spreading analysis also indicates that macrophages favor APTES-modified surfaces to dextranized or glass surfaces, with statistical differences present at 95% confidence levels using analysis of variance. Furthermore, comparing results for the two control surfaces, culture dish and glass, macrophages spread more on the culture dish than on the glass. That the hyaluronic acid-modified surface proved to be the least favorable for macrophage adhesion and spreading suggests that macrophage adhesion is favored by the cationic surfaces. This is further supported by the finding that the highest spreading occurred on the APTES-modified surface. Macrophage spread less on the anionic surface relative to the other surfaces in this study. This is consistent with studies by Brodbeck *et al.* who showed higher rates of apoptosis for macrophages adherent to anionic surfaces.[12,13]

Our results for cell clustering are also in close agreement with results of Gupta *et al.* showing that fibroblasts cultured on gels composed of hyaluronan and methylcellulose exhibit minimal cell attachment to the gel surface, with the majority of fibroblasts adhering to each other in clumps.[34] Additional studies have shown that mesenchymal stem cell spreading on hyaluronic acid hydrogels is directly proportional to the addition RGD peptides.[35] These results strongly suggest that hyaluronic acid by itself is a substrate that resists cellular attachment. Indeed our results presented here less macrophage attachment and spreading on hyaluronic surfaces than on the other materials tested.

While hyaluronic acid and dextran are both negatively charged polymers, the average macrophage spreading areas on these two surfaces are drastically different. This indicates that surface charge is not the only parameter dictating elements of the macrophage adhesion. Comparing the primary structure of the dextran and hyaluronic acid, both are found to be random coils[36,37] in solution. Detailed studies of hyaluronic acid using NMR have shown that it does have a more complex structure than the original picture. Scott and Heatley showed that hyaluronic acid has extensive hydrogen bonding that forces the polymer to form a 2-fold antiparallel helix structure with hydrophobic domains.[38,39] These helices form a tertiary structure, consisting of 2-fold helices in two planes at right angles bonded by hydrophobic interactions and hydrogen bonding. This suggests that the shape of hyaluronic acid also plays an important role in governing macrophage adhesion. Further studies on the structure of hyaluronic acid immobilized on surfaces will provide additional information regarding how the molecular structure modulates surface resistance to cellular adhesion.

Human macrophage adhesion is directed by surface micropatterning

In general, the cells did not align with any preferred orientation, but rather, they preferentially attached and spread on specific favorable surface chemistry. Studies have shown that cells can orient according to surface chemistry.[40–43] However, since the length scale of our surface chemical heterogeneity is on the micrometre length scale, a size scale which is comparable to, or larger than, the cells, specific cell orientation is not expected to occur.

On rhodamine-dextran/glass patterned surface, the cells did not preferentially attach or spread on the 90 μm square pattern or the 22 μm stripes, as is shown in Fig. 7A and 8A. This is expected and is consistent with the results of the spreading area analysis on the homogeneous surfaces. As shown in Fig. 6, the spreading areas are not statistically significantly different on the dextranized and glass surfaces. The macrophage adhesion on rhodamine-dextran/glass pattern is in agreement with the adhesion on the homogenous surfaces.

The fluorescein-hyaluronic acid pattern on glass shows some preferential attachment and spreading on the glass regions for the 90 μm square pattern and the 22 μm stripes, as is evident in Fig. 7B and 8B. The most dramatic preference is demonstrated by the rhodamine-dextran/fluorescein-hyaluronic acid for the 90 μm square patterned surface, which distinctly displays the success of using surface patterning to direct site-specific cell adhesion (Fig. 7C). In this binary polysaccharide pattern, most of the macrophages preferentially attach and spread onto the rhodamine-dextran regions and avoid adhering within the fluorescein-hyaluronic acid-modified area. This is similarly observed for the 22 μm stripes as shown in Fig. 8C. However, the preference is not as pronounced as the 90 μm square pattern because the width of the grid is 35 μm. It appears that the 22 μm width on the stripes is smaller than the size scale of the macrophages. Our observation of more favorable cell attachment and increased spreading on the patterned surface of hyaluronic acid/glass and the rhodamine-dextran/hyaluronic acid is consistent with several

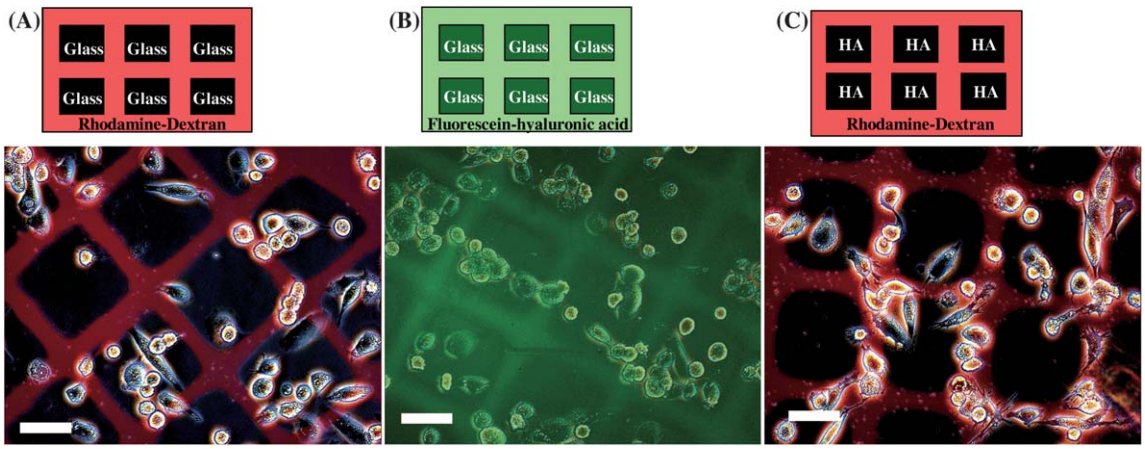

Fig. 7 Representative images of macrophage attachment and spreading on 90 μm square for (A) rhodamine-dextran/glass, (B) fluorescein-hyaluronic acid/glass and (C) rhodamine-dextran/hyaluronic acid patterns using the photodegradation method for 3 days. On the rhodamine-dextran pattern on glass, the macrophages have no preferential attachment or spreading. On the other hand, macrophages on the fluorescein-hyaluronic acid pattern on glass tend to attach and spread on the glass regions and only few cells are on the hyaluronic acid regions. The macrophages on the rhodamine-dextran and hyaluronic acid patterns show pronounced preferential attachment and spreading on the dextranized regions. Scale bar length is 50 μm.

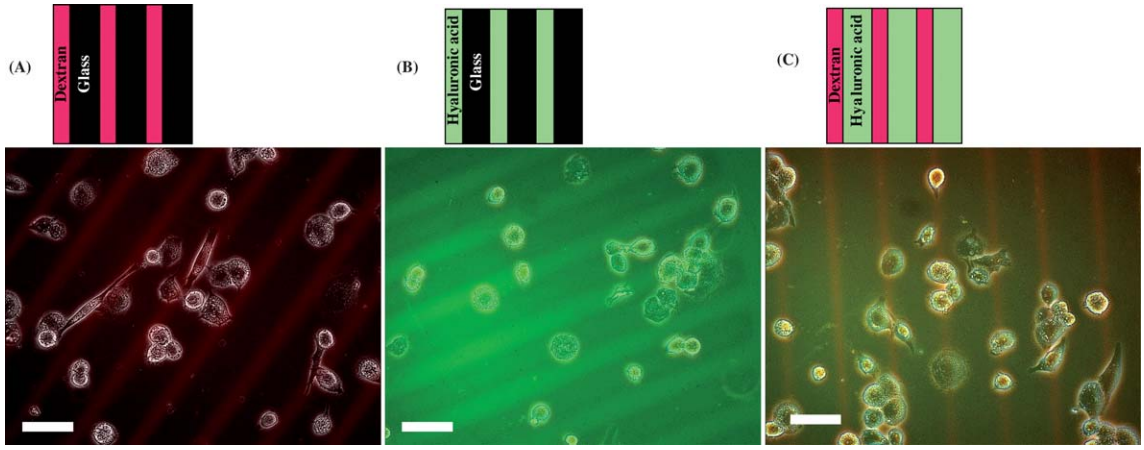

Fig. 8 Representative images of macrophage attachment and spreading on 22 μm stripes for (A) rhodamine-dextran/glass, (B) fluorescein-hyaluronic acid/glass and (C) rhodamine-dextran/hyaluronic acid patterns using the photodegradation method for 3 days. Similar to the square pattern, the macrophages on the 22 μm stripes of rhodamine-dextran pattern show no preferential attachment or spreading. On the fluorescein-hyaluronic acid pattern on glass or rhodamine-dextran and hyaluronic acid pattern, majority of the macrophages attach and spread on or close to the glass or dextranized regions, respectively. The 22 μm size appears to be smaller than the size of the macrophages, and thus, cells extend to the unfavorable regions of hyaluronic acid. Scale bar length is 50 μm.

cell studies on patterned surfaces involving cell lines such as fibroblasts,[44] epithelial cells,[45,46] endothelial cells[47,48] and macrophages.[11,49] This surface-directed cellular adhesion can serve as an excellent method to control inflammatory cell behavior for applications in tissue engineering, biomedical device development as well as diagnostic procedures and therapeutic interventions.

Conclusions

Microstamping and photodegradation methods were used successfully to create patterned surfaces bearing two polysaccharides, dextran and hyaluronic acid, which were then characterized and examined further in a biological model of inflammatory cell adhesion. Human macrophage THP-1 adhesion on patterned surfaces of dextran/glass, hyaluronic acid/glass and dextran/hyaluronic acid was evaluated. Hyaluronic acid-modified surfaces resisted macrophage adhesion relative to other surfaces studied, including the culture dish, glass, APTES and dextran. On the dextran/hyaluronic acid patterns, macrophages are surface-directed to the dextranized regions. Both surface chemistry and geometry can limit cell interaction with the coated region of the surface that more greatly favor cell adhesion. This is evidenced by the cell spreading area and the cell morphology. These findings are relevant to the fundamental understanding of cell–substrate interactions and development of the surfaces for anti-inflammatory response in biomedical applications.

Acknowledgements

This work was supported by NIH grants R01-HL060230 and T32-GM007612. RJC acknowledges partial support from NSF/

NSEC (DMR08-32802) and NSF/Polymer Program (DMR09-07493). Use of University of Pennsylvania Nano/Bio Interface Center AFM/TIRF instrument is acknowledged.

References

1 J. M. Squire, M. Chew, G. Nneji, C. Neal, J. Barry and C. Michel, *J. Struct. Biol.*, 2001, **136**, 239–255.
2 B. J. Ward and J. L. Donnelly, *Cardiovasc. Res.*, 1993, **27**, 384–389.
3 S. Weinbaum, X. B. Zhang, Y. F. Han, H. Vink and S. C. Cowin, *Proc. Natl. Acad. Sci. U. S. A.*, 2003, **100**, 7988–7995.
4 S. Reitsma, D. W. Slaaf, H. Vink, M. van Zandvoort and M. Egbrink, *Pflugers Archiv/European Journal of Physiology*, 2007, **454**, 345–359.
5 S. Weinbaum, J. M. Tarbell and E. R. Damiano, *Annu. Rev. Biomed. Eng.*, 2007, **9**, 121–167.
6 A. A. Constantinescu, H. Vink and J. A. E. Spaan, *Arterioscler., Thromb., Vasc. Biol.*, 2003, **23**, 1541–1547.
7 B. K. Chacko, R. Chandler, A. N. Mundhekar, H. M. Pruitt, A. Ramachandran, S. Barnes and R. P. Patel, *FASEB J.*, 2005, **19**, A776.
8 B. Wójciak-Stothard, A. Curtis, W. Monaghan, K. Macdonald and C. Wilkinson, *Exp. Cell Res.*, 1996, **223**, 426–435.
9 S. Lan, M. Veiseh and M. Q. Zhang, *Biosens. Bioelectron.*, 2005, **20**, 1697–1708.
10 T. O. Collier, J. M. Anderson, W. G. Brodbeck, T. Barber and K. E. Healy, *J. Biomed. Mater. Res., Part A*, 2004, **69**, 644–650.
11 K. M. DeFife, E. Colton, Y. Nakayama, T. Matsuda and J. M. Anderson, *J. Biomed. Mater. Res.*, 1999, **45**, 148–154.
12 W. G. Brodbeck, M. S. Shive, E. Colton, Y. Nakayama, T. Matsuda and J. M. Anderson, *J. Biomed. Mater. Res.*, 2001, **55**, 661–668.
13 W. G. Brodbeck, J. Patel, G. Voskerician, E. Christenson, M. S. Shive, Y. Nakayama, T. Matsuda, N. P. Ziats and J. M. Anderson, *Proc. Natl. Acad. Sci. U. S. A.*, 2002, **99**, 10287–10292.
14 D. S. Gray, J. L. Tan, J. Voldman and C. S. Chen, *Biosens. Bioelectron.*, 2004, **19**, 1765–1774.
15 Y. Ito, *Biomaterials*, 1999, **20**, 2333–2342.
16 A. L. DeMond and J. T. Groves, *Curr. Opin. Immunol.*, 2007, **19**, 722–727.
17 M. Goto, T. Tsukahara, K. Sato and T. Kitamori, *Anal. Bioanal. Chem.*, 2008, **390**, 817–823.
18 A. Bernard, J. P. Renault, B. Michel, H. R. Bosshard and E. Delamarche, *Adv. Mater.*, 2000, **12**, 1067–1070.
19 R. S. Kane, S. Takayama, E. Ostuni, D. E. Ingber and G. M. Whitesides, *Biomaterials*, 1999, **20**, 2363–2376.
20 A. Peramo, A. Albritton and G. Matthews, *Langmuir*, 2006, **22**, 3228–3234.
21 B. Wang, J. Feng and C. Y. Gao, *Macromol. Biosci.*, 2005, **5**, 767–774.
22 G. Zhang, X. Yan, X. L. Hou, G. Lu, B. Yang, L. X. Wu and J. C. Shen, *Langmuir*, 2003, **19**, 9850–9854.
23 C. S. Chen, M. Mrksich, S. Huang, G. M. Whitesides and D. E. Ingber, *Biotechnol. Prog.*, 1998, **14**, 356–363.
24 D. Y. Wang, Y. C. Huang, H. S. Chiang, A. M. Wo and Y. Y. Huang, *J. Biomed. Mater. Res., Part B*, 2007, **80**, 447–453.
25 Y. Zhou, O. Andersson, P. Lindberg and B. Liedberg, *Microchim. Acta*, 2004, **147**, 21–30.
26 G. P. Chen, Y. Ito, Y. Imanishi, A. Magnani, S. Lamponi and R. Barbucci, *Bioconjugate Chem.*, 1997, **8**, 730–734.
27 S. Alang Ahmad, A. Hucknall, A. Chilkoti and G. J. Leggett, *Langmuir*, 2010, **26**, 9937–9942.
28 Y. Lu, J. Sun and J. Shen, *Langmuir*, 2008, **24**, 8050–8055.
29 D. Miksa, E. R. Irish, D. Chen, R. J. Composto and D. M. Eckmann, *Biomacromolecules*, 2006, **7**, 557–564.
30 E. Ostuni, R. G. Chapman, E. R. Holmlin, S. Takayama and G. M. Whitesides, *Langmuir*, 2001, **17**, 5605.
31 I. Y. Tsai, N. Tomczyk, J. I. Eckmann, R. J. Composto and D. M. Eckmann, *Colloids Surf., B*, 2011, **84**, 241–252.
32 S. Martwiset, A. E. Koh and W. Chen, *Langmuir*, 2006, **22**, 8192–8196.
33 M. C. C. Ferrer, S. Yang, D. M. Eckmann and R. J. Composto, *Langmuir*, 2010, **26**, 14126–14134.
34 D. Gupta, C. H. Tator and M. S. Shoichet, *Biomaterials*, 2006, **27**, 2370–2379.
35 Y. Lei, S. Gojgini, J. Lam and T. Segura, *Biomaterials*, 2011, **32**, 39–47.
36 J. Sabatie, L. Choplin, J. L. Doublier, J. Arul, F. Paul and P. Monsan, *Carbohydr. Polym.*, 1988, **9**, 287–299.
37 T. C. Laurent and J. R. E. Fraser, *FASEB J.*, 1992, **6**, 2397–2404.
38 J. E. Scott and F. Heatley, *Biomacromolecules*, 2002, **3**, 547–553.
39 J. E. Scott and F. Heatley, *Proc. Natl. Acad. Sci. U. S. A.*, 1999, **96**, 4850–4855.
40 I. Y. Tsai, A. J. Crosby and T. P. Russell, *Cell Mechanics*, 2007, **83**, 67–87.
41 B. J. Papenburg, E. D. Rodrigues, M. Wessling and D. Stamatialis, *Soft Matter*, 2010, **6**, 4377–4388.
42 M. Mrksich, L. E. Dike, J. Tien, D. E. Ingber and G. M. Whitesides, *Exp. Cell Res.*, 1997, **235**, 305–313.
43 M. Veiseh, O. Veiseh, M. C. Martin, F. Asphahani and M. Q. Zhang, *Langmuir*, 2007, **23**, 4472–4479.
44 I. Y. Tsai, M. Kimura, R. Stockton, J. A. Green, R. Puig, B. Jacobson and T. P. Russell, *J. Biomed. Mater. Res., Part A*, 2004, **71**, 462–469.
45 A. S. Andersson, J. Brink, U. Lidberg and D. S. Sutherland, *IEEE Trans. NanoBiosci.*, 2003, **2**, 49–57.
46 S. J. Liliensiek, S. Campbell, P. F. Nealey and C. J. Murphy, *J. Biomed. Mater. Res., Part A*, 2006, **79**, 185–192.
47 N. Okochi, T. Okazaki and H. Hattori, *Langmuir*, 2009, **25**, 6947–6953.
48 N. Zheng, P. Yang, Q. Y. Wang, Z. H. Yang and N. Huang, *Sci. China, Ser. E: Technol. Sci.*, 2010, **53**, 257–263.
49 H. Sahlin, R. Contreras, D. F. Gaskill, L. M. Bjursten and J. A. Frangos, *J. Biomed. Mater. Res., Part A*, 2006, **77**, 43–49.

